



**HAL**  
open science

## Streptococcus pyogenes Cas9 ribonucleoprotein delivery for efficient, rapid and marker-free gene editing in Trypanosoma and Leishmania

Corinne Asencio, Perrine Hervé, Pauline Morand, Quentin Oliveres, Chloé Alexandra Morel, Valérie Prouzet-Mauleon, Marc Biran, Sarah Monic, Mélanie Bonhivers, Derrick Roy Robinson, et al.

### ► To cite this version:

Corinne Asencio, Perrine Hervé, Pauline Morand, Quentin Oliveres, Chloé Alexandra Morel, et al.. Streptococcus pyogenes Cas9 ribonucleoprotein delivery for efficient, rapid and marker-free gene editing in Trypanosoma and Leishmania. Molecular Microbiology, 2024, 121 (6), pp.1079-1094. 10.1111/mmi.15256 . hal-04616877

HAL Id: hal-04616877

<https://hal.science/hal-04616877>

Submitted on 19 Jun 2024


**HAL** is a multi-disciplinary open access archive for the deposit and dissemination of scientific research documents, whether they are published or not. The documents may come from teaching and research institutions in France or abroad, or from public or private research centers.

L'archive ouverte pluridisciplinaire **HAL**, est destinée au dépôt et à la diffusion de documents scientifiques de niveau recherche, publiés ou non, émanant des établissements d'enseignement et de recherche français ou étrangers, des laboratoires publics ou privés.



Distributed under a Creative Commons Attribution 4.0 International License

# *Streptococcus pyogenes* Cas9 ribonucleoprotein delivery for efficient, rapid and marker-free gene editing in *Trypanosoma* and *Leishmania*

Corinne Asencio<sup>1</sup> | Perrine Hervé<sup>1</sup> | Pauline Morand<sup>1</sup> | Quentin Oliveres<sup>1</sup> |  
Chloé Alexandra Morel<sup>1</sup> | Valérie Prouzet-Mauleon<sup>2</sup> | Marc Biran<sup>3</sup> | Sarah Monic<sup>1</sup> |  
Mélanie Bonhivers<sup>1</sup> | Derrick Roy Robinson<sup>1</sup> | Marc Ouellette<sup>4</sup> | Loïc Rivière<sup>1</sup> |  
Frédéric Bringaud<sup>1</sup> | Emmanuel Tetaud<sup>1</sup> 

<sup>1</sup>Univ. Bordeaux, CNRS, MFP, UMR 5234, Bordeaux, France

<sup>2</sup>Univ. Bordeaux, CNRS/INSERM, TBMCORE/CRISP<sup>2</sup>edit, UAR 3427/US005, Bordeaux, France

<sup>3</sup>Univ. Bordeaux, CNRS, CRMSB, UMR 5536, Bordeaux, France

<sup>4</sup>Centre de Recherche en Infectiologie du Centre de Recherche du CHU de Québec, Département de Microbiologie, Infectiologie et Immunologie, Faculté de Médecine, Université Laval, Québec, Québec, Canada

## Correspondence

Emmanuel Tetaud, CNRS, MFP, UMR 5234, Univ. Bordeaux, Bordeaux F-33000, France.  
Email: [emmanuel.tetaud@u-bordeaux.fr](mailto:emmanuel.tetaud@u-bordeaux.fr)

## Funding information

Fondation pour la Recherche Médicale, Grant/Award Number: EQU201903007845; IDEX; Canadian Institutes of Health Research; Centre National de la Recherche Scientifique; Université de Bordeaux; Agence Nationale de la Recherche, Grant/Award Number: ANR-11-LABX-0024, ANR-20-CE91-0003, ANR19-CE15-0004-01 and ANR-19-CE17-0014-03

## Abstract

Kinetoplastids are unicellular eukaryotic flagellated parasites found in a wide range of hosts within the animal and plant kingdoms. They are known to be responsible in humans for African sleeping sickness (*Trypanosoma brucei*), Chagas disease (*Trypanosoma cruzi*), and various forms of leishmaniasis (*Leishmania* spp.), as well as several animal diseases with important economic impact (African trypanosomes, including *Trypanosoma congolense*). Understanding the biology of these parasites necessarily implies the ability to manipulate their genomes. In this study, we demonstrate that transfection of a ribonucleoprotein complex, composed of recombinant *Streptococcus pyogenes* Cas9 (*SpCas9*) and an in vitro-synthesized guide RNA, results in rapid and efficient genetic modifications of trypanosomatids, in marker-free conditions. This approach was successfully developed to inactivate, delete, and mutate candidate genes in various stages of the life cycle of *T. brucei* and *T. congolense*, and *Leishmania* promastigotes. The functionality of *SpCas9* in these parasites now provides, to the research community working on these parasites, a rapid and efficient method of genome editing, without requiring plasmid construction and selection by antibiotics but requires only cloning and PCR screening of the clones. Importantly, this approach is adaptable to any wild-type parasite.

## KEYWORDS

CRISPR/Cas9, efficiency, kinetoplastids, marker-free, protist, ribonucleoprotein complex transfection, universal

Corinne Asencio and Perrine Hervé co-first authors.

This is an open access article under the terms of the [Creative Commons Attribution](https://creativecommons.org/licenses/by/4.0/) License, which permits use, distribution and reproduction in any medium, provided the original work is properly cited.

© 2024 The Authors. *Molecular Microbiology* published by John Wiley & Sons Ltd.

## 1 | INTRODUCTION

In the realm of modern molecular biology, few innovations have captured the world's attention like CRISPR-Cas9. The CRISPR-Cas9 system has catapulted molecular biology into a new era of precision gene editing and genetic engineering. CRISPR (Clustered Regularly Interspaced Short Palindromic Repeats) and CRISPR-associated protein 9 (CRISPR-Cas9) is a revolutionary genome-editing technology that has unlocked unprecedented opportunities for precise manipulation of the genetic code. Since its discovery in the early 2000s (Barrangou et al., 2007; Mojica et al., 2005), CRISPR-Cas9 has rapidly evolved into a game-changing tool with the potential to transform medicine, agriculture, biotechnology, and various other fields (Jinek et al., 2012). This groundbreaking system is derived from a remarkable natural defense mechanism found in bacteria and archaea, allowing researchers to edit, correct, or modify genes with accuracy and efficiency that was previously unimaginable (Barrangou et al., 2007; Ishino et al., 1987; Mojica et al., 2005).

This technology was very quickly used to study trypanosomatids, which are unicellular eukaryotic flagellate parasites that affect millions of people and animals worldwide (Peng et al., 2014). In humans, they are responsible for African sleeping sickness (Human African trypanosomiasis), Chagas disease (American trypanosomiasis), and leishmaniasis in South America, Africa, India, the Mediterranean region, and the Middle East. Animal African Trypanosomiasis, including Nagana, are debilitating disease affecting livestock, primarily cattle in sub-Saharan Africa. Nagana, which is caused by *Trypanosoma congolense*, *Trypanosoma vivax*, and *Trypanosoma brucei brucei*, leads to severe health issues, including anemia, weight loss, and decreased productivity in infected animals, making it a significant economic and agricultural concern in affected regions (Desquesnes et al., 2022). Understanding the biology of these parasites necessarily requires the ability to manipulate their genomes. Before the development of the CRISPR-Cas9 system, genome modification was achieved through homologous recombination using resistance markers for selection, or by RNA interference, but only in *T. brucei* (Ngo et al., 1998) and *T. congolense* (Coustou et al., 2012; Inoue et al., 2002) as *T. cruzi* and some *Leishmania* do not share the RNA interference machinery (Kolev et al., 2011). It is noteworthy, however, that *Leishmania* subgenus *Vianna* still has functional RNA interference machinery (Lye et al., 2022). Because of genome diploidy, deletion/inactivation of genes proved to be time-consuming and conditioned by the limited number of available antibiotic resistance markers. This is even more true in *Leishmania* spp., where a high frequency of aneuploidy is frequently observed (Imamura et al., 2016; Mannaert et al., 2012; Rogers et al., 2011).

The CRISPR-Cas9 system has been now employed to modify the genomes of *T. brucei*, *T. cruzi*, and *Leishmania* spp. with a rapidly growing number of publications (founding articles are: Beneke et al., 2017; Kovarova et al., 2022; Lander et al., 2015, 2016, 2017; Peng et al., 2014; Rico et al., 2018; Shaw et al., 2020; Sollelis

et al., 2015; Zhang et al., 2017; Zhang & Matlashewski, 2015). In most studies, Cas9 or Cas9-gRNA complexes are endogenously expressed after transfection of the parasites and selection with antibiotic resistance markers. However, constitutive expression of Cas9 has shown, in rare cases, genomic instability (Boutin et al., 2021; Zhang et al., 2017) and could lead to a decrease in cell growth (Peng et al., 2014; Ryan et al., 2014). Conditional expression of Cas9, as described in *T. brucei*, is helpful in overcoming this issue (Kovarova et al., 2022; Rico et al., 2018). Another issue with the CRISPR-Cas9 system is the potential off-target genome disruption (Fu et al., 2013). The transient expression of guide RNAs, combined with the constitutive expression of Cas9 and a repair DNA construct, represents a possibility to limit off-target effects and reduce other potential undesirable effects associated with Cas9 targeting. The ongoing development of new, increasingly accurate Cas9 variants, should also limit this problem. Interestingly, CRISPR-mediated editing can be achieved by transfecting cells with *in vitro*-generated Cas9 protein/guide RNA complexes. As recombinant Cas9 is rapidly eliminated after transfection, this approach, which limits potential off-targets (D'Astolfo et al., 2015) and reduces toxicity issues (Kim et al., 2014; Liang et al., 2015), has proven to be particularly efficient in *T. cruzi* and *Plasmodium* sp. (Crawford et al., 2017; Soares Medeiros et al., 2017). This method is straightforward, fast, and highly efficient, as it does not require gene cloning and minimizes the use of selection markers. However, genome modification with *in vitro*-generated Cas9 protein/guide RNA complexes in *T. cruzi*, *Leishmania* spp., and *T. brucei* relies, in the study by Soares Medeiros et al. (2017), exclusively on the use of a smaller Cas9, isolated from *Staphylococcus aureus* (SaCas9) (Soares Medeiros et al., 2017). The same authors also reported that Cas9 isolated from *Streptococcus pyogenes* (SpCas9), despite being the most commonly used and commercialized, does not function in these parasites, and the lack of activity appears to be due to the larger size of SpCas9 compared to SaCas9, which is approximately 40kDa smaller (Soares Medeiros et al., 2017).

In this study, we have demonstrated that SpCas9 is fully functional after transfection of the Cas9/gRNA complex in both the bloodstream (BSF) and procyclic (PCF) forms of *T. brucei* and *T. congolense*, as well as in the promastigotes of *Leishmania infantum*. This Cas9/gRNA complex can be delivered into cells, with or without a repair sequence, to inactivate, mutate, or tag candidate genes, without the need for selection markers and with very high efficiency. The functionality of SpCas9 in these parasites now provides the research community working on these parasites a rapid and efficient method for genome edition without requiring gene cloning and/or selection, that only requires cloning of modified cell lines. The key point of this approach is the generation of homozygous clones with high efficiency in a single round of transfection. It will also allow genome editing of cells that are difficult to cultivate or whose cell density is too low to envisage using conventional techniques, such as field isolates. Finally, this approach should be adaptable to all kinetoplastids and, importantly, any transfectable cell type.

## 2 | RESULTS

### 2.1 | The SpCas9/RNP complex is functional for genome editing activity

Soares Medeiros et al. described in *T. cruzi*, *T. brucei* and *Leishmania* the unexpected result that exogenous ribonucleoprotein Cas9 from *Streptococcus pyogenes* (SpCas9, 163 kDa) was not functional after transfection, in contrast to the smaller *Staphylococcus aureus* Cas9 (SaCas9, 124 kDa) (Soares Medeiros et al., 2017). Since SpCas9 is fully active when endogenously expressed (Lander et al., 2015; Peng et al., 2014; Sollelis et al., 2015; Zhang & Matlashewski, 2015), it was proposed that ribonucleoprotein SpCas9 complexes are not internalized by electroporation in trypanosomatids. To revisit these data, we tried to inactivate a constitutively expressed cytosolic GFP in *T. brucei* PCF using extracellular RNP complexes composed of SpCas9 and guide RNAs (gRNAs). The guide RNAs consist of an optimized and chemically modified Alt-R CRISPR-Cas9 crRNA specifically designed to target the gene of interest, complexed with a tracrRNA, a conserved 67-nt RNA sequence essential for forming the guide RNA recognized by *S. pyogenes* Cas9. All guide RNAs are from Integrated DNA Technologies (IDT). We used the commercial SpCas9 from IDT (Alt-R™ SpCas9 Nuclease 3NLS) and three gRNAs targeting different sequences of the GFP gene (Table S1). GFP expression was monitored by flow cytometry at 24, 48, and 72 h post-transfection with the RNP complexes (Figure 1a).  $5 \times 10^5$  GFP-expressing *T. brucei* PCF cells were subjected to electroporation with 20  $\mu$ g of gRNA-loaded SpCas9 (GFP1, 2, or 3), or gRNA only as a control (GFP2). Unexpectedly, transfection of GFP-expressing PCF without SpCas9 (Figure 1a—Top left panel) resulted in a very strong drop in fluorescence after 24 h for about 50% of the population, probably related to the electroporation conditions. However, 48 h later, GFP expression recovered to its initial level (Figure 1a—Top left panel). Importantly, a strong decrease in fluorescence occurred immediately after transfection with GFP1, GFP2, and GFP3 gRNA-loaded SpCas9, which did not recover to its initial level after 72 h (Figure 1a—gRNA GFP1, GFP2, and GFP3), indicating that a significant portion of cells did not express active GFP anymore. It is noteworthy that GFP1 and GFP2 gRNA are more efficient at inactivating GFP expression than GFP3 gRNA (Figure 1a—Bar chart) and the efficiency depends on the amount of RNP complex transfected (1.5-fold increase in GFP-negative cells with a 3-fold increase in GFP2 gRNA-loaded SpCas9) (Figure 1a—Bar chart).

To confirm that the decrease in GFP expression is indeed caused by Cas9/gRNA-dependent GFP gene inactivation, we cell-sorted and cloned cells failing to express GFP and sequenced the DNA region targeted by the GFP2 guide RNA used (Figure 1c). As expected, a 33-bp deletion at the gRNA targeting site was observed in all GFP-negative cells (Figure 1c). The deleted region is flanked by two 8-bp homologous sequences, which suggests a repair of double-strand breaks by the microhomology-mediated end-joining (MMEJ) pathway as previously described in *T. cruzi* and

*Leishmania* (Peng et al., 2014; Zhang et al., 2017). These data show that the commercial SpCas9 from IDT is fully functional in our experimental protocols and suggest that the size of the exogenous ribonucleoprotein complex is not a limiting factor, contrary to the hypothesis made for *T. cruzi*. The only difference that we could identify between the IDT SpCas9 and the one used by Soares Medeiros et al. (2017) is the number of nuclear localization signals (NLS), three versus two, suggesting that the lack of activity in *T. cruzi* could be explained by weak nuclear targeting of the complex after transfection.

In order to produce our own in-house recombinant Cas9 protein, we constructed a recombinant DNA SpCas9 sequence (eSpCas9, a rationally engineered Cas9 with improved specificity (Slaymaker et al., 2016)) containing three NLS regions, that is, one at the N-terminus and two at the C-terminus of the protein, plus two polyhistidine tracts to allow the purification of the expressed recombinant protein by chromatography (Figure 1b). The protein was expressed and purified in *E. coli* (Cf. Experimental procedures, Figure S1) and its activity was assayed by replacing the IDT SpCas9 with the eSpCas9 in the GFP2 gRNA/Cas9 complex. As expected, the purified eSpCas9 is able to dose-dependently inactivate GFP expression (Figure 1b). Note that above 40  $\mu$ g of eSpCas9, there is no further decrease in GFP expression (Figure 1b, right). Sequencing of the GFP gene in cloned cell lines confirmed the inactivation of the gene by a 33-bp deletion. A larger 97-bp deletion flanked by two 6-bp homologous regions was also detected in clone Bc3 (Figure 1c). It is worth noting that the presence of polyhistidine tracts, one each at the N and C-terminal of the protein, does not appear to affect Cas9 activity. We concluded that the edition of PCF *T. brucei* genes with SpCas9/gRNA complexes is functional and the use of laboratory-produced eSpCas9 is equally effective as the commercial SpCas9 (IDT).

### 2.2 | Development of a marker-free approach for editing the genomes of T. brucei PCF and BSF

Cas9-mediated double-strand DNA breaks can be repaired by homology-directed repair (HDR), as long as an appropriate repair template is provided (Peng et al., 2014). We have tested this by inactivating the *TbFis1* gene (Tb927.10.8660), in both *T. brucei* PCF and BSF using marker-dependent and marker-free approaches. *TbFis1* protein is a potential homolog of the mitochondrial fission factor identified in yeast, Fis1p (Mozdy et al., 2000), which enables the recruitment of the dynamin Dnm1 to the mitochondria and triggers mitochondrial fission. The first approach consists of inserting a repair template encoding a resistance gene (in this case against phleomycin, *BleR*) flanked by 5' and 3' regulatory sequences and a short homology region of the *TbFis1* gene flanking the Cas9-cleavage site (50 bp) (Figure 2a). Cells were cloned after 8 to 12 days of culture in the presence of phleomycin. The correct insertion of the repair DNA fragment was controlled by PCR and sequencing, as shown in Figure 2b,c. After Cas9-mediated

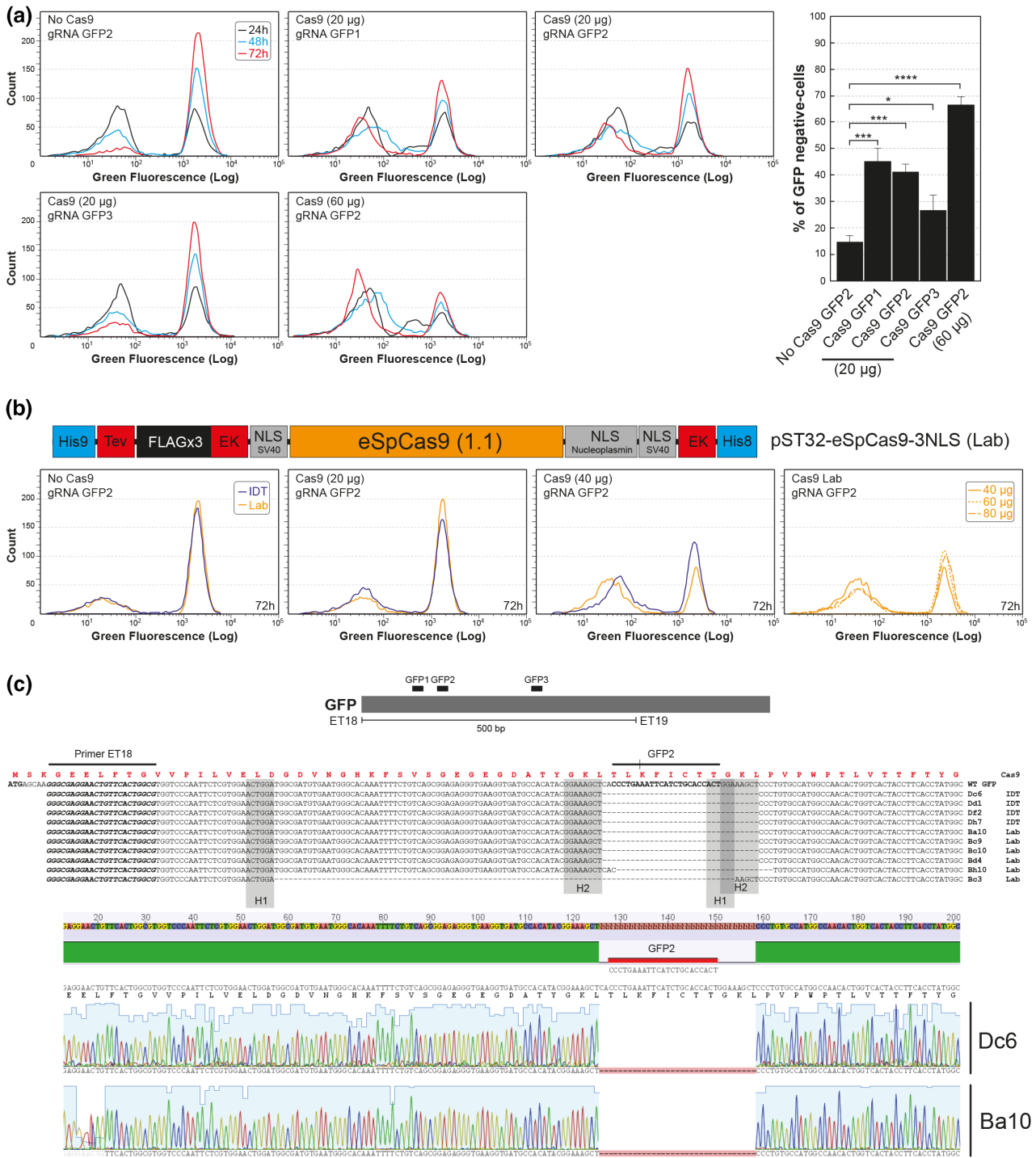


**FIGURE 1** GFP inactivation in *T. brucei* PCF. (a) Fluorescence flow cytometry analysis of *T. brucei* constitutively expressing a cytosolic eGFP. GFP fluorescence was monitored over time from 24 to 72 h after transfection with 20  $\mu$ g (no Cas9, Cas9/gRNA GFP1, Cas9/gRNA GFP2, Cas9/gRNA GFP3) or 60  $\mu$ g (Cas9/gRNA GFP2) of RNP complexes from IDT, and a bar chart showing the percentage of GFP-negative cells at 72 h after transfection with the different guides ( $n = 3$ ). Prism software was employed for statistical analysis, utilizing *t*-tests (unpaired, normal distribution, parametric test, and two-tailed). The significance levels (*p* values) are represented by asterisks. (b) The top panel shows a schematic representation of the plasmid allowing eSpCas9 expression in *E. coli*. The blue boxes represent the two polyhistidine sequences at the N and C-termini of the protein, the red boxes represent the cleavage sites of TEV and enterokinase (EK) proteases, the gray boxes represent the three nuclear localization signals (NLS), the black box represents three repeats of the FLAG epitope and the orange box represents the eSpCas9 coding sequence. The bottom panel shows the fluorescence flow cytometry analysis of *T. brucei* expressing the GFP monitored at 72 h after transfection with RNPs complexes from IDT or laboratory-purified (Lab) (no Cas9, 20  $\mu$ g Cas9/gRNA GFP2, 40  $\mu$ g Cas9/gRNA GFP2, 40, 60, and 80  $\mu$ g Cas9/gRNA GFP2). (c) Sequence comparison of a portion of the GFP gene from clones no longer expressing GFP. The sequence shows only the region targeted by the GFP2 guide RNA. The gray boxes (H1 and H2) highlight the homology regions probably used for repair by MMEJ. Sequences resulting from inactivation by laboratory-purified Cas9 and those from commercial Cas9 are labeled Lab and IDT, respectively. Below is shown the corresponding chromatogram of the Dc6 and Ba10 clones (Confidence interval 95%—*p*-value style: 0.1234 (ns); 0.0332 (\*); 0.0021 (\*\*); 0.0002 (\*\*\*); <0.0001 (\*\*\*\*)).

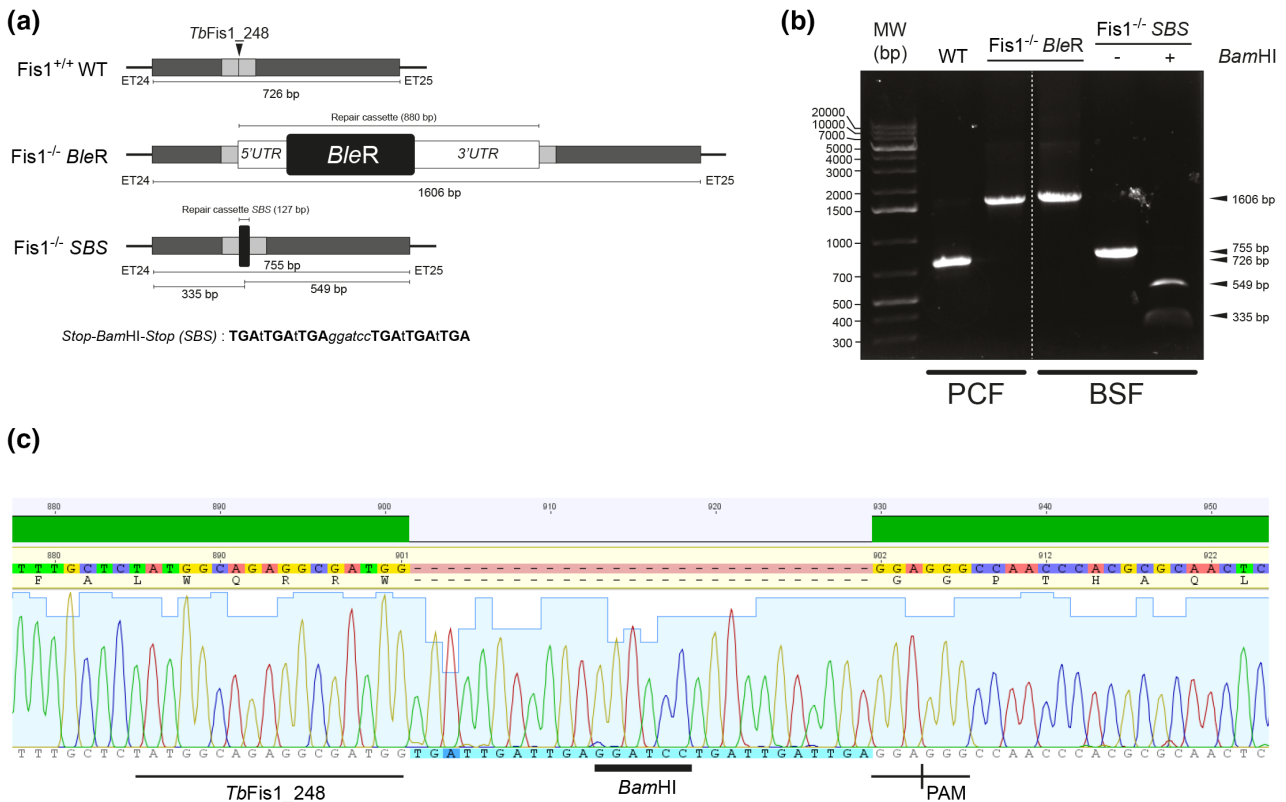


**FIGURE 2** Inactivation of the *TbFis1* gene in both *T. brucei* PCF and BSF. (a) Schematic representation of the *TbFis1* locus and the two inactivation strategies by inserting the phleomycin resistance marker (*BleR*) or a short sequence containing a succession of stop codons (SBS). The position of the guide RNA is indicated by a vertical arrow (*TbFis1\_248*) and the 50-bp flanking sequences allowing repair through HDR are shown in gray. The 5' and 3' untranslated regions (UTRs) are depicted as white boxes. (b) PCR confirmation of *TbFis1* gene inactivation on both alleles in PCF and BSF cells (the gel shows the PCR results of a single PCF and a single BSF clone among the various clones tested). PCR products (primer ET24/ET25) are directly analyzed on agarose gel (*Fis1*<sup>-/-</sup> *BleR*) or after its digestion with *Bam*HI (*Fis1*<sup>-/-</sup> SBS), allowing easy discrimination of gene inactivation on both alleles. (c) Chromatogram of the *TbFis1* sequence highlighting the insertion of the SBS cassette.

recombination, the size of the targeted *TbFis1* gene increased by 880bp, which corresponds to the size of the repair cassette (Figure 2b). Both alleles encoding *TbFis1* (homozygotes) were targeted in 100% of PCF clones but in only 10% of BSF clones (Figure 2b). The 90% remaining BSF clones had a single allele inactivated (heterozygotes) (Table 1).

The second approach consists of inserting a shorter repair cassette composed of stop codons in all three reading frames and a restriction site absent in the targeted gene (here *Bam*HI), flanked by short regions of homology corresponding to 50-bp flanking the Cas9-cleavage site (Figure 2a–SBS). The *Bam*HI restriction site enables rapid discrimination of repair template integration on one or two alleles after PCR and digestion with *Bam*HI. Under these marker-free conditions, cells were cloned 1 to 3 days after transfection and insertion of the repair cassette was tested by PCR/*Bam*HI digestion and sequencing (Figure 2b–SBS). 3% and 4% of the BSF clones tested were inactivated on both alleles or one allele only, respectively (Table 1). Obtaining a large number of homozygous mutants confirms that the *TbFis1* gene is not essential for PCF and BSF growth. Incidentally, the inactivation of the *TbFis1* gene did not induce a change in mitochondrial structure (Figure S2A,B).

### 2.3 | Inactivation of a *T. brucei* multigene family by *SpCas9*

Genetic manipulation of trypanosomatids is often difficult when a high number of resistance markers are required, as exemplified by the sequential inactivation of several genes or when multigene families are addressed (Reis-Cunha et al., 2018). We, therefore, tested whether transfection, with the gRNA/RNP complex, is also effective for the inactivation of a multigene family, here the one encoding glycerol kinase (GK) in *T. brucei* PCF. RNAi-mediated down-regulation of GK expression has shown that, in standard growth conditions, this non-essential gene family is required to metabolize glycerol in *T. brucei* PCF and BSF (Allmann et al., 2021; Pineda et al., 2018). GK is encoded by 11 tandemly arranged copies distributed over the two alleles, containing five and six copies, respectively (Figures 3a and S3A,B). We tested a single gRNA targeting the entire multigenic family and a repair cassette including the phleomycin resistance marker (*BleR*) (Figure 3a). The fate of the allelic GK gene clusters after transfection and selection with phleomycin was tested by PCR using primers flanking the Cas9 recognition site. All the tested phleomycin-resistant clones (11 clones) showed the presence of a single ~1500-bp band corresponding to the parental allele (616bp) inactivated by insertion of the repair cassette (880bp),

TABLE 1 Summary of the various CRISPR/Cas9 inactivation experiments.

Gene targeted	Parasite	Inactivation cassette	Numbers of tested clones	Homozygous	Heterozygous	Both alleles inactivated (%)
Fis1	<i>T. brucei</i> PCF	<i>BleR</i> +3'/5'UTR	5	5	0	100
	<i>T. brucei</i> BSF		12	1	11	8
	<i>T. brucei</i> BSF	<i>PacR</i> without UTR	34	0	33	0
	<i>T. brucei</i> BSF	SBS	76	2	3	3
GK	<i>T. brucei</i> PCF	<i>BleR</i> +3'/5'UTR	11	11	0	100
ALDH	<i>L. infantum</i> Pro	<i>PacR</i> without UTR	39	12	1	31
	<i>L. infantum</i> Pro	<i>mRED</i> without UTR	6	5	1	83
	<i>L. infantum</i> Pro	SBS	12	4	0	33
LysoPLA	<i>T. congolense</i> BSF	<i>BleR</i> +3'/5'UTR	4	4	0	100
	<i>T. congolense</i> PCF	SBS	5	3	0	60
GK	<i>T. congolense</i> BSF	<i>BleR</i> +3'/5'UTR	4	3	1	75
Gene targeted	Parasite	Inactivation cassette	GFP negative cells tested	WT GFP	Mutated GFP	Inactivated cells (%)
GFP <sup>a</sup>	<i>T. brucei</i> PCF	None	16	3	13	81

Abbreviation: SBS, a short sequence containing a succession of stop codons.

<sup>a</sup>The GFP gene was integrated into a single allele in the genome, and the selection of clones was based on the absence of fluorescence.

suggesting that GK genes are inactivated (Figure 3b, Table 1). This was confirmed by a Southern-blot analysis with the GK probe after digestion of the genomic DNA with a restriction enzyme present once in each of the GK repeat units (*KpnI*), which generated a 5197-bp band corresponding to the GK copy located at the 5' end of both allelic clusters (two copies) plus an intense 3582-bp band corresponding to the other GK genes (nine copies) (Figure 3a,c). As expected, the genome of all the tested mutant cell lines contains two *KpnI* bands-containing GK whose size is increased by ~800bp, corresponding to the length of the repair cassette. It is noteworthy that, following cleavage by Cas9 in the same locus, it is likely that several GK copies were deleted by homologous recombination. Indeed, a Southern blot analysis of genomic DNA digested by *MfeI* (which is absent in the GK repeat units), revealed a significant reduction of the size of one GK allelic cluster in the 1B10, 2G2, and 2F11 clones (Figure S3). As expected, a western blot analysis with the anti-GK immune serum showed that GK expression is abolished in all the analyzed mutant cell lines, confirming that they are bona fide GK null mutants (GK<sup>-/-</sup>) (Figure 3d). In addition, glycerol metabolism is abolished in the GK<sup>-/-</sup> cell lines, as shown by quantitative

proton NMR spectrometry analyses of the <sup>13</sup>C-enriched end products excreted from the metabolism of uniformly <sup>13</sup>C-enriched glycerol ([U-<sup>13</sup>C]-glycerol) (Allmann et al., 2021; Bringaud et al., 2015; Pineda et al., 2018). Indeed, the parental PCF *T. brucei* convert [U-<sup>13</sup>C]-glucose or [U-<sup>13</sup>C]-glycerol to <sup>13</sup>C-enriched acetate and succinate. In contrast, the excretion of <sup>13</sup>C-enriched end products from [U-<sup>13</sup>C]-glycerol is abolished in the GK<sup>-/-</sup> 2E6 cell line, while the metabolism of [U-<sup>13</sup>C]-glucose is unaffected (Figure 3e). Taken together, these data demonstrate the high efficiency of a single transfection with gRNA/SpCas9 complexes to inactivate all copies of a large multigene family.

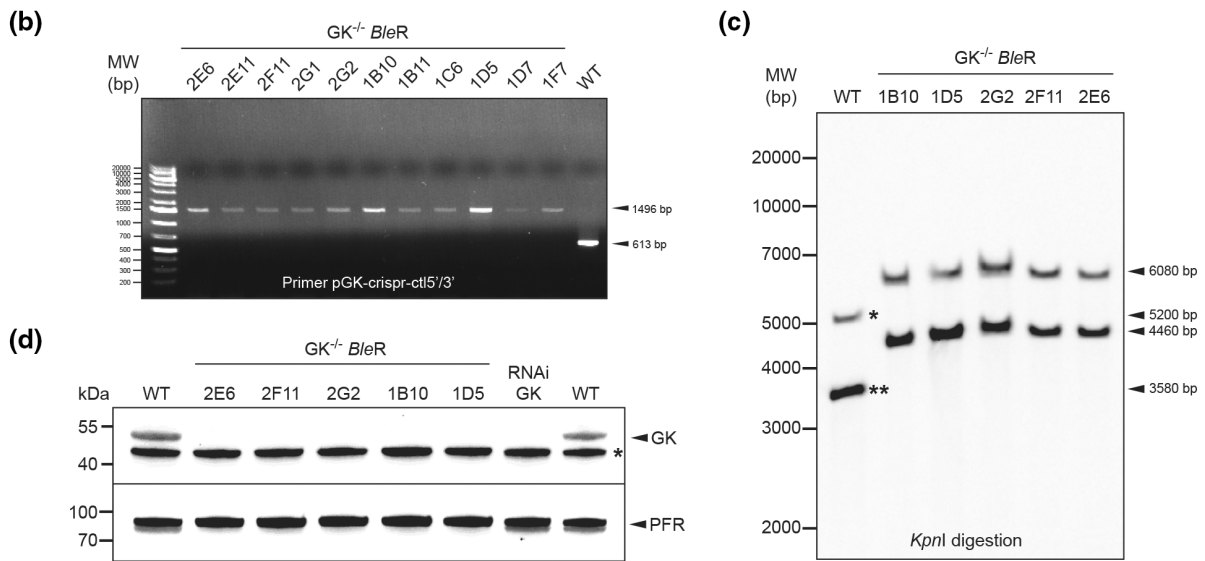
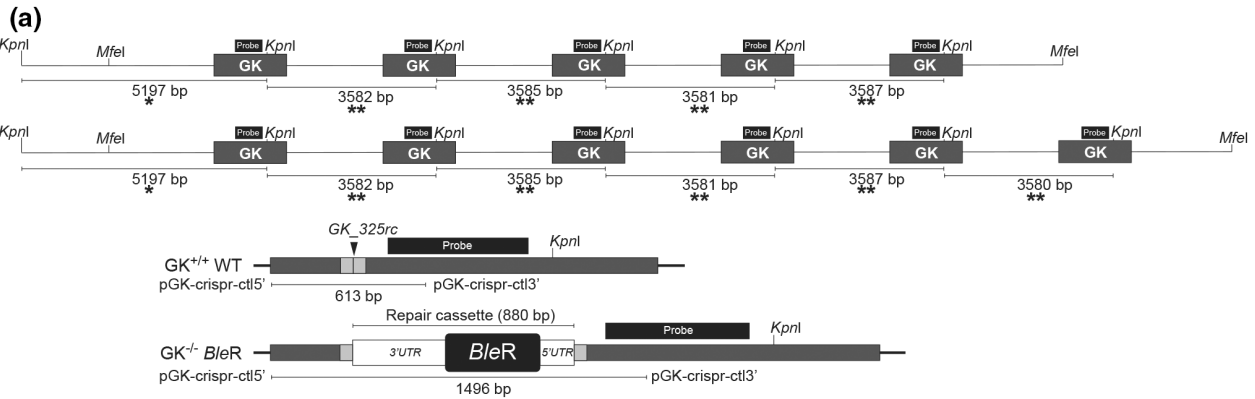
## 2.4 | SpCas9 is also functional in other trypanosomatids

We also tested the efficiency of RNP complex delivery to edit the genome of the promastigote forms of *Leishmania infantum* and of the bloodstream and procyclic forms of *T. congolense*. Several approaches have been used to inactivate the gene encoding ALDH, the

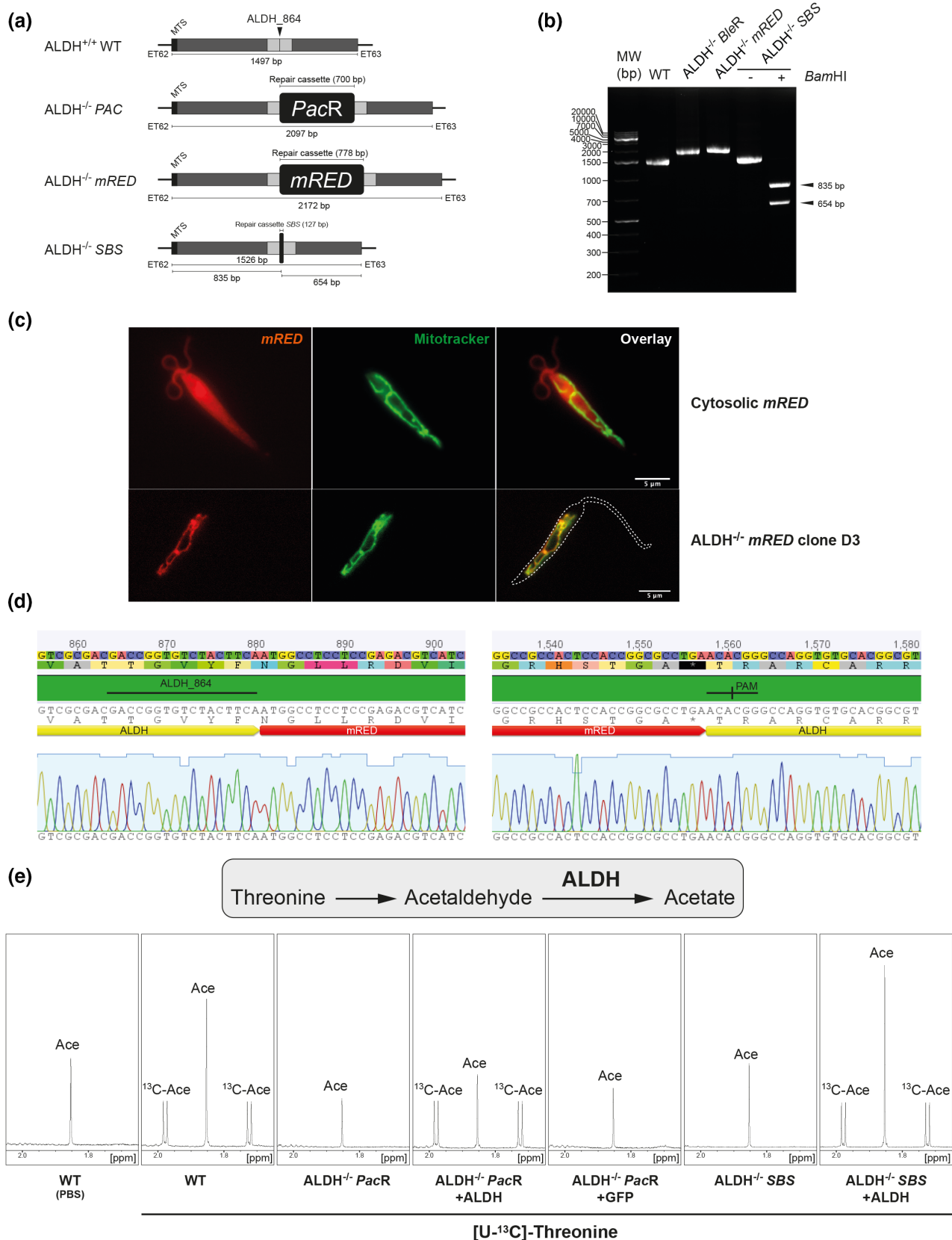
**FIGURE 3** Inactivation of the multigenic family encoding the glycerol kinase (GK) in *T. brucei* PCF. (a) Schematic representation of the two alleles of the GK family in *T. brucei* and the inactivation strategy used by insertion of the phleomycin resistance marker *BleR*. The position of the guide RNA is indicated by a vertical arrow (GK\_325rc) and the 50-bp flanking sequences allowing repair through HDR are shown in gray. The 5' and 3' untranslated regions (UTRs) are depicted as white boxes. The position of the probe used for the southern-blot analysis is indicated by a black box. (b) Confirmation by PCR of GK gene inactivation on both alleles in PCF. PCR products from various phleomycin-resistant clones (primer pGK-crispr-ctl5'/pGK-crispr-ctl3') are analyzed on an agarose gel. (c) Southern blot analysis of various phleomycin-resistant clones. The two bands detected in the parental cells (WT) correspond to the GK copy located at the 5' extremity of the clusters (one asterisk) and to all the other GK copies (two asterisks). The insertion of the resistance marker increases the size of both of these bands by 880bp in the phleomycin-resistant clones. (d) Western blot analysis of whole-cell extracts from different phleomycin-resistant *T. brucei* PCF clones. RNAi targeting GK was included as a control (Pineda et al., 2018). The band revealed below the GK (indicated by an asterisk) is due to cross-reactivity with another protein (Pineda et al., 2018). Antibodies against the paraflagellar rod (PFR) were used as a loading control. (e) <sup>1</sup>H-NMR analysis of <sup>13</sup>C-enriched end products (succinate and acetate, <sup>13</sup>C-Suc, and <sup>13</sup>C-Ace, respectively) excreted from the metabolism of [U-<sup>13</sup>C]-glucose and [U-<sup>13</sup>C]-glycerol, by the parental (WT) and clone 2E6 (GK<sup>-/-</sup>) PCF cells. A portion of each spectrum ranging from 1.6 to 2.6 ppm is presented.

mitochondrial enzyme responsible for converting acetaldehyde to acetate in *L. infantum* promastigotes (LINF\_250017300, ALDH), using a SpCas9/gRNA complex targeting the ALDH sequence and various

repair cassettes. Here we used repair cassettes to insert (i) a puromycin resistance marker (*PacR*), (ii) a fluorescent protein (monomeric RED, mRED), and (iii) a short sequence containing stop codons and







a *Bam*HI restriction site (SBS) as described above (Figure 4a). After transfection, clones were selected either by addition of puromycin (PacR cassette, ALDH<sup>-/-</sup> PAC cells), by cell cytometry at 595/613 nm (mRED cassette, ALDH<sup>-/-</sup> mRED cells) or by PCR and sequencing

after cell cloning (SBS cassette, ALDH<sup>-/-</sup> SBS cells). In each condition, the insertion of the repair cassette was checked by PCR with primers flanking the insertion site (Figure 4a,b). We were able to obtain homozygous mutant clones for each repair cassette, with efficiencies

**FIGURE 4** ALDH inactivation in *L. infantum* promastigote. (a) Schematic representation of the *ALDH* locus and the three inactivation strategies used, that is, insertion of the puromycin resistance marker (*PacR*), of the monomeric RED fluorescent protein (*mRED*) or of a short sequence containing a succession of stop codons (*SBS*). The position of the guide RNA is indicated by a vertical arrow (*ALDH\_864*) and the 50-bp flanking sequences allowing repair through HDR are shown in gray. (b) Confirmation by PCR of *ALDH* gene inactivation on both alleles. PCR products from phleomycin-resistant, RED fluorescent and *SBS* clones (primer ET62/ET63) are analyzed on an agarose gel. In the case of the *SBS* strategy, the PCR product was digested by *Bam*HI. (c) mRED fluorescence was used to localized the chimeric *ALDH/mRED* (*ALDH*<sup>-/-</sup> *mRED*, clone D3) and compared with the cytosolic expression of mRED. Mitochondrial localization of the chimeric protein was confirmed by labeling the cells with Mitotracker Green FM (Invitrogen). (d) Portion of the chromatogram showing the fusion of the mRED sequence with the *ALDH* sequence. (e) <sup>1</sup>H-NMR analysis of <sup>13</sup>C-enriched end products (<sup>13</sup>C-acetate, <sup>13</sup>C-Ace) excreted from metabolism of [U-<sup>13</sup>C]-threonine metabolism by the parental (WT), *ALDH*<sup>-/-</sup> *PacR* clone 1B1 re-expressing (*ALDH*<sup>-/-</sup> *PacR* +*ALDH*) or not the *ALDH* genes and *ALDH*<sup>-/-</sup> *SBS* clone A1 re-expressing (*ALDH*<sup>-/-</sup> *PacR* +*ALDH*) or not the *ALDH* gene. A rescue control was performed by expressing GFP in the *ALDH*<sup>-/-</sup> *PacR* clone. A portion of each spectrum ranging from 1.65 to 2.05 ppm is presented.

ranging from 30% (*ALDH*<sup>-/-</sup> *SBS* cells) to 83% (*ALDH*<sup>-/-</sup> *mRED* cells) (Table 1). It should be noted that the *PacR* and *mRED* cassettes are only composed of the corresponding ORF inserted in frame with the *ALDH* coding sequence (Figure 4a). The *mRED* protein exhibited a fluorescence pattern resembling that of mitochondria, similar to Mitotracker labeling, in the *ALDH*<sup>-/-</sup> *mRED* cell line, in contrast to the cytosolic-like pattern observed when *mRED* was expressed using an expression vector. This suggests that the mitochondria-targeting motif at the N-terminus of the *ALDH* protein directed the chimeric *ALDH/mRED* protein to the mitochondria (Figure 4c,d). To confirm that both *ALDH* alleles were indeed inactivated, we quantified the product of the *ALDH* enzymatic reaction, that is, acetate, which is excreted in the medium from the metabolism of threonine. As expected, the production of <sup>13</sup>C-enriched acetate is abolished in the *ALDH*<sup>-/-</sup> *PAC* clone 1B1, as shown by proton NMR spectrometry analysis of the <sup>13</sup>C-enriched end products excreted from the metabolism of [U-<sup>13</sup>C]-threonine (Figure 4e) (Bringaud et al., 2015). Integrating an ectopic copy of the *ALDH* encoding gene in an *ALDH*<sup>-/-</sup> *PAC* cell line restored <sup>13</sup>C-enriched acetate production from the metabolism of [U-<sup>13</sup>C]-threonine, as opposed to expression of GFP (Figure 4e). Similarly, the *ALDH*<sup>-/-</sup> *SBS* mutant (clone A1) no longer excretes <sup>13</sup>C-enriched acetate from the metabolism of [U-<sup>13</sup>C]-threonine (Figure 4e).

To test this approach in *T. congolense*, we targeted the *LysoPLA* gene (TcIL3000.A.H\_000623300), which is a non-essential gene encoding an excreted lysophospholipase in *T. brucei* (Monic et al., 2022; Tounkara et al., 2021). Repair cassettes containing either the phleomycin-resistant gene (*BleR*) flanked by 5' and 3' regulatory sequences or the marker-free *SBS* sequence were used to transfect BSF and PCF, respectively (Figure 5a). As above, the insertion of the repair cassettes was checked by PCR and sequencing from genomic DNA isolated from Phleomycin selection (*BleR* cassette) or cell cloning (*SBS* cassette). The four BSF clones tested are all homozygous mutants, further confirmed by western blot analyses using an anti-*LysoPLA* immune serum showing that *LysoPLA* is no longer expressed (Figure 5a-c). Similarly, three out of the five PCF clones tested are homozygous mutants (Figure 5d, clones 1B6, 1E10, and 2C3), as confirmed by western blot analyses (Figure 5e).

We also used *SpCas9* to inactivate the *GK* multigene family in *T. congolense*, which is composed of three *GK* copies per allele, one of which is a pseudogene with two frameshifts (Figure 6a,

TcIL3000\_0\_55170, TriTrypDB). BSF were transfected with a *SpCas9/gRNA* complex and a repair *BleR* cassette containing 5' and 3' regulatory sequences. Among the four clones tested, three were homozygote mutants and one was heterozygote (Figure 6b). The absence of *GK* expression was confirmed by western blot analyses using anti-*GK* antibodies (Figure 6c) and by quantitative proton NMR spectrometry analyses of excreted end products from the metabolism of [U-<sup>13</sup>C]-glycerol and glucose (Figure 6d). Indeed, the production of <sup>13</sup>C-enriched succinate and acetate from the metabolism of [U-<sup>13</sup>C]-glycerol is abolished in a mutant cell line, while the conversion of non-enriched glucose to succinate and acetate is not affected (Figure 6d). In conclusion, our data clearly showed that transfection of RNP complexes containing *SpCas9* has the capacity to rapidly and efficiently modify all members of multigene families in *T. congolense* and probably all trypanosomatids.

### 3 | DISCUSSION

Since 2014, the majority of kinetoplastid studies using CRISPR/Cas9 technology have employed parasites that constitutively express Cas9. In the case of *Trypanosoma* species, this necessitated genome integration of the RNP-encoding gene, and in some instances, gRNAs into the genome. More recently, Soares Medeiros et al. (2017) demonstrated that transfection of the Cas9-gRNA RNP complex also induced rapid and efficient genome editing in kinetoplastids, but only with a Cas9 derived from *Staphylococcus aureus* and hypothesized that *SpCas9* was too large to be transfected and functional (Soares Medeiros et al., 2017). In this current study, we demonstrate that *SpCas9* is fully functional and effective after transfection into the parasites. We demonstrated that both the commercial *SpCas9* (IDT) and the *SpCas9* produced in our laboratory enable rapid and efficient genome modification in various kinetoplastids, including *T. brucei* and *T. congolense*, across different life cycle stages (insect and mammalian stages), as well as *Leishmania* promastigotes.

We have shown that both the commercial *SpCas9* (IDT) and the *SpCas9* produced in our laboratory enable rapid and efficient genome modification in several kinetoplastids including *T. brucei* and *T. congolense*, across different life cycle stages (insect and mammalian stages) and *Leishmania* promastigotes. We were able to target single genes and multigene families.

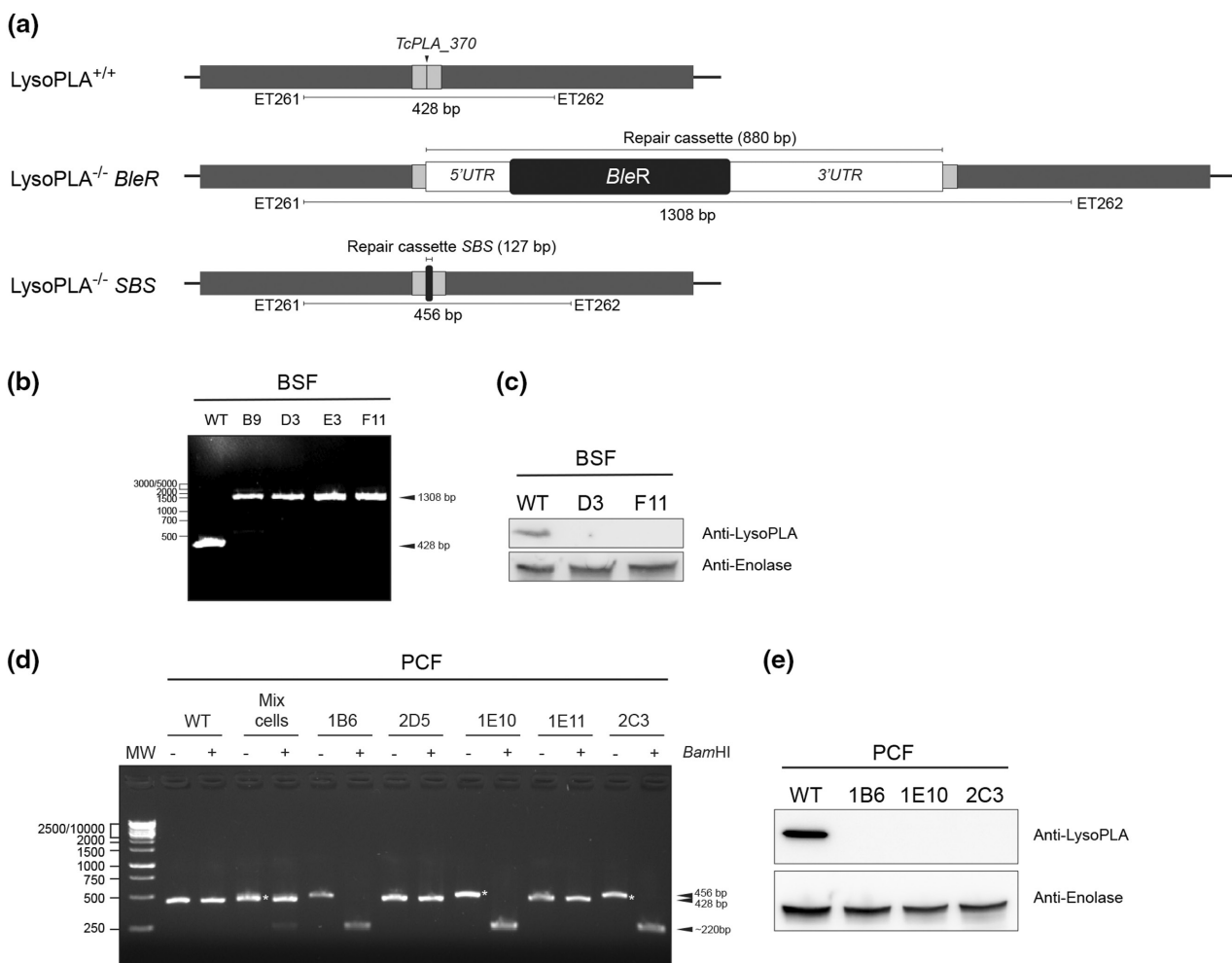
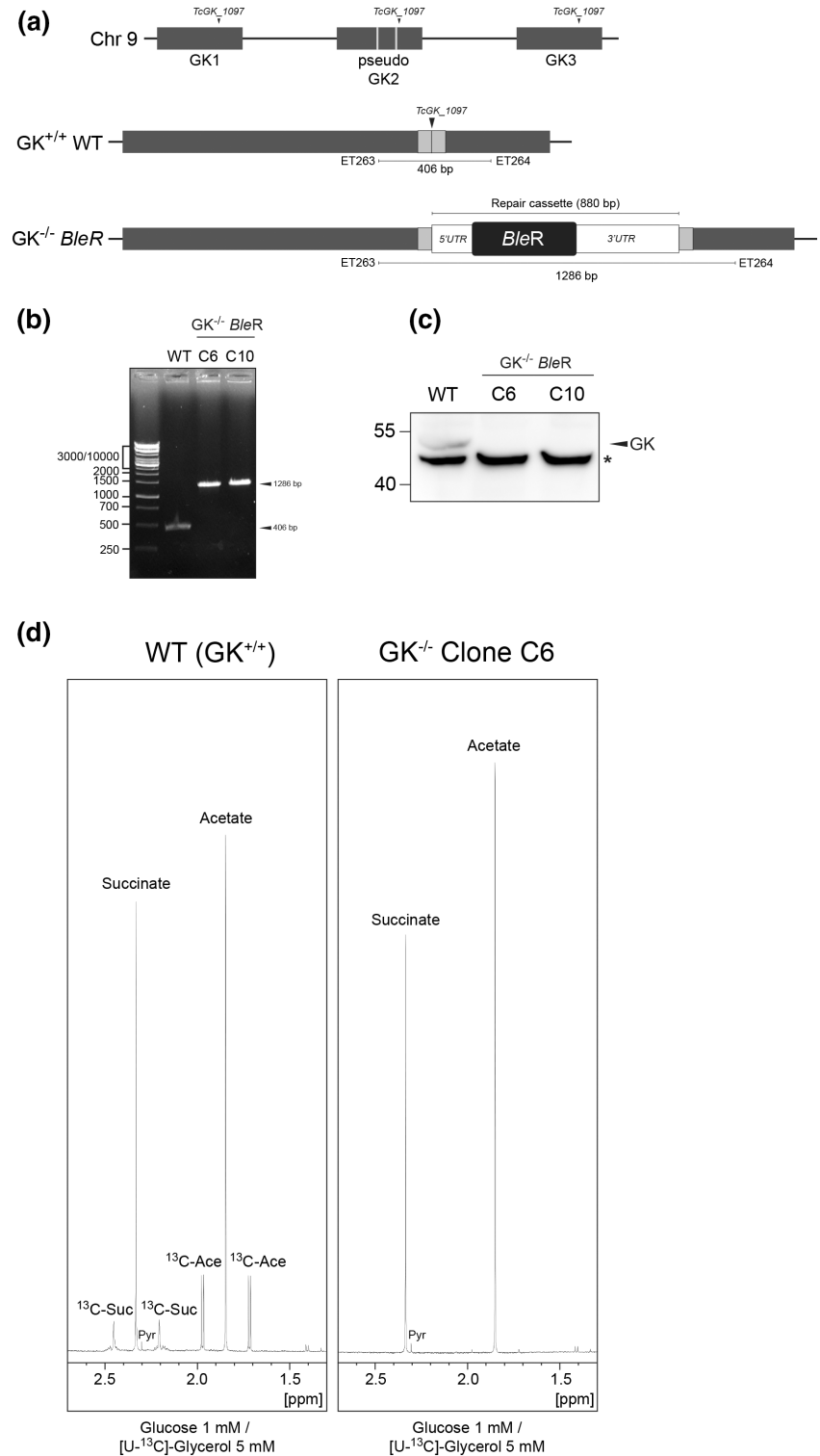


**FIGURE 5** Inactivation of the *LysoPLA* in *T. congolense* BSF and PCF. (a) Schematic representation of the *LysoPLA* locus in *T. congolense* and the two inactivation strategies used, that is, insertion of the phleomycin resistance marker (*BleR*) or a short sequence containing a succession of stop codons (SBS). The position of the guide RNA is indicated by a vertical arrow (*TcPLA\_370*) and the 50-bp flanking sequences allowing repair through HDR are shown in gray. The 5' and 3' untranslated regions (UTRs) are depicted as white boxes. (b) Confirmation of *LysoPLA* gene inactivation on both alleles in *T. congolense* BSF cells, by PCR analysis of various phleomycin-resistant clones (primer ET261/ET262). (c) Western blot analysis of whole-cell extracts from two phleomycin-resistant *T. congolense* BSF clones. Antibodies against enolase were used as a loading control. (d) Confirmation of *LysoPLA* gene inactivation on both alleles in *T. congolense* PCF cells by agarose gel analysis of *Bam*HI-digested PCR products from various phleomycin-resistant clones (primer ET261/ET262). The "Mix cells" lane corresponds to the cell population before cloning, containing parental cells, and heterozygous and homozygous mutants. The asterisk indicates the 456-bp band, which does include a *Bam*HI restriction site. Clones 2D5 and 1E11 exhibit the wild-type profile. (e) Western blot analysis of whole-cell extracts from marker-free (SBS) *T. congolense* PCF clones. Antibodies against enolase were used as a loading control.

This approach based on transfection of RNP complexes offers several advantages including, (i) adaptability to any laboratory, (ii) for non-essential genes, both alleles are inactivated simultaneously, which is also valid for large multigene families, (iii) Cas9 remains transiently in the transfected cell, preventing them from the deleterious effect of constitutive Cas9 expression, and (iv) no need for selection markers, which implies that numerous modifications can be achieved in the same cell line. Peng et al. (2014) demonstrated that mutations induced by Cas9 were mediated by MMEJ, a process that results in a deletion between homologous regions (Peng et al., 2014). The prediction of MMEJ sites is made very easy through the Eukaryotic Pathogen CRISPR guide RNA/DNA Design Tool (EuPaGDT) website (Peng & Tarleton, 2015). Enabling the optional

search for microhomology allows for the exploration of microhomology pairs bracketing each gRNA. These microhomology pairs can facilitate the joining of double-stranded breaks even in the absence of a repair template. We have also observed such deletions in *T. brucei* with both the commercial *SpCas9* (from IDT) and laboratory-produced *SpCas9*, in the absence of repair cassettes. This approach proved to be very efficient since we successfully inactivated the sole allele of the *GFP* gene introduced in *T. brucei* PCF with an efficiency close to 50%, all within a few days. When double-strain breaks through Cas9 are combined with repair cassettes, it becomes easy to achieve targeted insertions through HDR, allowing inactivation or tagging of genes at their endogenous loci. We have thus been able to insert resistance markers (*BleR* and *PacR*), a gene encoding

**FIGURE 6** Inactivation of the multigenic family encoding the glycerol kinase (GK) in *T. congolense* BSF. (a) Schematic representation of the GK locus and its inactivation by inserting the phleomycin resistance marker *BleR*. The position of the guide RNA is indicated by a vertical arrow (*TcGK\_1097*) and the 50-bp flanking sequences allowing repair through HDR are shown in gray. The 5' and 3' untranslated regions (UTRs) are depicted as white boxes. (b) PCR confirmation of *GK* gene inactivation on both alleles in two different BSF clones. (c) Western blot analysis of whole-cell extracts from two phleomycin-resistant *T. congolense* BSF clones. The band revealed below the GK (indicated by an asterisk) is due to cross-reactivity with another protein. (d)  $^1\text{H}$ -NMR analysis of end products (succinate and acetate) excreted from the metabolism of glucose and  $[\text{U-}^{13}\text{C}]$ -glycerol by the parental (WT) and clone C6 ( $\text{GK}^{-/-}$ ) BSF cell lines. A portion of each spectrum ranging from 1.3 to 2.7 ppm is presented. In the NMR experiments, *T. congolense* BSF were incubated in the presence of a mixture of D-glucose (1 mM) and D- $[\text{U-}^{13}\text{C}]$ -glycerol (5 mM) to keep them alive. Resonances were assigned as follows: Ace, acetate;  $^{13}\text{C}$ -Ace,  $^{13}\text{C}$ -enriched acetate; Suc, succinate;  $^{13}\text{C}$ -Suc,  $^{13}\text{C}$ -enriched succinate; Pyr, pyruvate.



the RED fluorescent protein, or a short insertion sequence containing a series of stop codons enabling the inactivation of the target gene. We did not test the limit for the homology arms' size, but in *T. cruzi* and *Leishmania*, approximately 30bp is sufficient (Beneke et al., 2017; Espada et al., 2021; Soares Medeiros et al., 2017; Zhang et al., 2017; Zhang & Matlashewski, 2015). Finally, the insertion of short coding sequences at the 5' and/or 3' ends of the targeted genes (in order to tag them) can be achieved on both alleles without

a selection marker and without significant modification of the UTRs (Morel et al., 2023). In terms of efficiency, there appears to be no set rule, that is, it may depend on the gRNA, the targeted gene, the stage of division, and how the parasites are selected. It should be noted that we tested, in *T. brucei* PCF, inactivation cassettes containing or not regulatory sequences at the 5' and 3' ends of the genes used for selection (in this case, phleomycin). In both cases (with or without UTR), we obtained resistant clones. This suggests that in

the absence of regulatory sequences at the 5' and 3' ends of the resistance gene, it is expressed from the regulatory sequences of the inactivated gene. This is also the case in *Leishmania*, where we obtained cells resistant to phleomycin but also fluorescent with mRED expression. In this latter case, the gene encoding mRED is in phase with the N-terminal sequence of the ALDH protein, resulting in a chimeric protein targeting the mRED to the mitochondria but inactivating the ALDH protein (Table 1). In *T. cruzi*, successive transfections appear to significantly increase efficiency (Soares Medeiros et al., 2017), and this is an interesting approach when homozygous clones are not obtained. Here, we consistently obtained homozygous clones for non-essential genes. However, for genes suspected to be essential, only heterozygous clones could be obtained. Thus, the consistent acquisition of exclusively heterozygous clones after successive transfections could suggest the potential essentiality of the gene. Confirming this hypothesis will be necessary through other approaches, such as RNA interference (RNAi), for example. It should be noted that successive transfections may also lead to the selection of chromosomal polysomy in *Leishmania* (Tovar et al., 1998).

Another important point to consider is the optimization of Cas9 for its importation by electroporation. Soares Medeiros et al. (2017) reported that recombinant *SpCas9* is not active on *T. cruzi*, which was interpreted as non-internalization by electroporation due to a size issue (Soares Medeiros et al., 2017). In agreement with their hypothesis, they showed the functionality of a smaller Cas9 (Cas9 from *Staphylococcus aureus*), which is abolished by fusion with GFP (Soares Medeiros et al., 2017). However, the recombinant *SpCas9* is functional in the same experimental set-up. The only difference between the recombinant *SpCas9* used by Soares Medeiros et al. (2017) and us is the presence of 2 and 3 NLS sequences, respectively. These data suggest that the size of the ribonucleoprotein complex is not a limiting factor, however, the number of NLS sequences to achieve effective nuclear targeting seems to be an important factor to consider. Very recently, Minet et al. also managed to transfect and modify *T. congolense* bloodstream forms using a commercial *SpCas9*, which contains three NLS in its sequence, further demonstrating that this protein is fully functional in kinetoplastids (Minet et al., 2023).

Finally, this system is likely functional in all cells that can be transfected, enabling more relevant studies on field strains. Indeed, this system is also valuable for studying cells that are difficult to cultivate (low cell density) and that previously required a significant number of cells for transfection through classical homologous recombination approaches. We used  $5 \times 10^5$  cells to efficiently edit both alleles of the targeted genes, but we believe that this approach could be adapted to many fewer cells, provided that a sufficient number of clonal cells are sorted by flow cytometry. The transfection of the RNP-gRNA complex and its various derivatives, including dead Cas9, dCas9-methyltransferases, activators, etc., presents a wealth of exciting research opportunities across diverse cell types (Engstler & Beneke, 2023; Goma et al., 2022). Notably, this approach holds great promise for advancing our understanding of biological processes showing several redundant pathways, such as some metabolic capacities

(Millieroux et al., 2018; Wargnies et al., 2018), for which the need to inactivate multiple enzymes has often been hampered by the scarcity of selection markers.

## 4 | EXPERIMENTAL PROCEDURES

### 4.1 | Trypanosomes and cell cultures

The procyclic forms (PCF) of *T. brucei* EATRO1125.T7T (TetR-HYG-T7RNAPOL-NEO, where TetR stands for tetracycline resistance, HYG for hygromycin, T7RNAPOL for RNA polymerase T7, and NEO for neomycin) was cultured at 27°C with 5% CO<sub>2</sub> in SDM79 medium containing 10% (vol/vol) heat-inactivated fetal calf serum, 5 µg/mL hemin, 0.04 mg/mL streptomycin, 40 U/mL penicillin (SigmaP4333), 25 µg/mL hygromycin, and 10 µg/mL neomycin. The bloodstream forms (BSF) of *T. brucei* 427 90-13 (TetR-HYG-T7RNAPOL-NEO) was cultured at 37°C with 5% CO<sub>2</sub> in Iscove's modified Dulbecco's medium (IMDM) supplemented with 10% (vol/vol) heat-inactivated fetal calf serum, 0.2 mM β-mercaptoethanol, 36 mM NaHCO<sub>3</sub>, 1 mM hypoxanthine, 0.16 mM thymidine, 1 mM sodium pyruvate, 0.05 mM bathocuproine, 1.5 mM L-cysteine, 5 µg/mL hygromycin, and 2.5 µg/mL neomycin. *L. infantum* 263 promastigote form was cultured at 27°C with 5% CO<sub>2</sub> in SDM79 medium containing 10% (vol/vol) heat-inactivated fetal calf serum, 5 µg/mL hemin, 0.04 mg/mL streptomycin, and 40 U/mL penicillin (SigmaP4333). The BSF of *T. congolense* IL3000 was cultured at 34°C with 5% CO<sub>2</sub> in MEM medium (Sigma M0643) containing 20% (vol/vol) heat-inactivated goat serum (InvitroGen 16210072), 6 mg/mL HEPES, 2 mg/mL NaHCO<sub>3</sub>, 1 mg/mL glucose, 100 µg/mL sodium pyruvate, 10 µg/mL adenosine, 14 µg/mL hypoxanthine, 4 µg/mL thymidine, 14 µg/mL bathocuproine, 2 mM glutamine and 0.2 mM β-mercaptoethanol, pH 7.2-7.4. The PCF of *T. congolense* was cultured at 27°C with 5% CO<sub>2</sub> in MEM medium (Sigma M0643) containing 20% (vol/vol) heat-inactivated fetal calf serum, 6 mg/mL HEPES, 2 mg/mL NaHCO<sub>3</sub>, 5 µg/mL hemin, 2 mM glutamine and 8 mM Proline, pH 7.3-7.4. Growth was monitored by daily cell counting with the cytometer Guava® Muse® or Guava® easyCyte™.

### 4.2 | CRISPR/Cas9 inactivation

Gene inactivation was achieved by inserting double-stranded DNA corresponding either to a resistance marker (phleomycin or puromycin), to a gene encoding a fluorescent protein (monomeric RED), or to a short sequence containing six successive stop codons in the three reading phases and a *Bam*HI restriction site. These double-stranded DNA fragments were also flanked by 50bp homologous to the 5' and 3' sequences of the Cas9 cut site. Prior to transfection, equal quantities (0.4 µmol each) of TracrRNA and gRNA from IDT were combined. The mixture was then heated at 95°C for 5 min and gradually cooled to room temperature. Subsequently, this mixture was combined with 30 µg of *SpCas9* sourced from IDT (Alt-RTM *SpCas9*

Nuclease 3NLS, Catalog #1074181) or purified in the laboratory.  $5 \times 10^5$  cells were respectively transfected, using Amaxa nucleofector II (100  $\mu$ L), with 1  $\mu$ g of purified cassette (phleomycin or puromycin resistance marker, mRED or StopBamHIStop in a final volume of 10  $\mu$ L) and 30  $\mu$ g of Cas9 protein preloaded with the mixture of TracrRNA and gRNA. Cells were transfected using program X-001 for *T. brucei* PCF and BSF or U-033 for *L. infantum* promastigote and *T. congolense* PCF and BSF and resuspended in 5 mL of medium containing or not phleomycin (for *T. brucei* PCF 5  $\mu$ g/mL or BSF 2.5  $\mu$ g/mL and for *T. congolense* PCF 2.5  $\mu$ g/mL or BSF 5  $\mu$ g/mL) or puromycin (*T. brucei* PCF 1  $\mu$ g/mL and *Leishmania* promastigote 100  $\mu$ g/mL). Following a 2-day culture period, a portion of the transfected cells underwent DNA extraction using the NucleoSpin Blood kit (Macherey-Nagel) followed by PCR amplification using primers that flank the Cas9 cleavage site (Table S1). Gel analysis of the PCR products is expected to show two bands corresponding to the wild-type and modified gene, as illustrated in Figure 5d for mixed cells. Cells were subsequently cloned using a cell sorter (TBM Core facility), and the selection of inactivated cells was performed by DNA extraction using the NucleoSpin Blood kit (Macherey-Nagel) followed by PCR amplification using primers flanking the Cas9 cleavage site as previously described. Guide RNA was designed using EuPaGDT (Peng & Tarleton, 2015), from <http://tritypdb.org>. Primers and guide RNA used were synthesized by Integrated DNA Technologies (IDT) and listed in Tables S1 and S2.

### 4.3 | Southern blot

A total of 2.5  $\mu$ g of genomic DNA from *T. brucei* (EATRO1125.T7T) were subjected to *KpnI* or *MfeI* digestion, electrophoresed in 0.8% agarose gel, blotted onto Hybond N<sup>+</sup> membrane (Amersham), and hybridized with labeled probe at 50°C in 6X SSPE (1X SSPE: 0.18M NaCl, 10mM NaH<sub>2</sub>PO<sub>4</sub>, 1mM ethylenediaminetetraacetate, pH7.0), 0.1% SDS and washed at 50°C using 0.5X SSPE-0.1% SDS, before revelation. Probes were obtained by PCR using the primers pGK-S55 and pGK-S53 (Table S1) and labeled with the PCR DIG Probe Synthesis Kit (Roche) according to the manufacturer and revealed using the DIG Luminescent Detection Kit and DIG Easy Hyb (Roche).

### 4.4 | Western blot

Total protein extracts ( $5 \times 10^6$  cells) were separated by SDS-PAGE (10%) and immunoblotted on TransBlot Turbo Midi-size PVDF Membranes (Bio-Rad). Immunodetection was performed using the primary antibodies, diluted in PBS-Tween-Milk (0.05% Tween20, 5% skimmed milk powder), rabbit anti-GK (1:1000), rabbit anti-LysoPLA (1:1000) and mouse anti-enolase (1:100,000, gift from P.A.M. Michels, Edinburgh, UK). Revelation was performed using a second antibody coupled to the HRP (anti-rabbit or anti-mouse IgG conjugated to horseradish peroxidase, Bio-Rad, 1:5000 dilution) and detected using the Clarity Western-enhanced chemiluminescence (ECL) substrate as describes

by the manufacturer (Bio-Rad). Images were acquired and analyzed with the ImageQuant Las 4000 luminescent image analyzer.

### 4.5 | Mitochondria staining on living cells

Mitotracker Green FM (10nM, MP07510 from Invitrogen) was added to cells previously washed with PBS ( $5 \times 10^6$ – $1 \times 10^7$  cells per mL) for 10min at room temperature, then cells were washed twice with PBS and spread on slides. Images were acquired with MetaMorph software on Zeiss Axioplan 2 microscope and processed with ImageJ.

### 4.6 | Immunofluorescence

Cells were washed twice with PBS, then fixed with 2% paraformaldehyde (PFA) for 10min at room temperature and 0.1mM glycine was added for 10min to stop the reaction. The cells were spread on slides and permeabilized with 0.05% triton X-100. After incubation in PBS containing 4% bovine serum albumin (BSA) for 20min, cells were incubated for 1h with primary antibodies diluted in PBS-BSA 4%, washed four times with PBS and incubated for 45min with secondary antibodies diluted in PBS-BSA 4% followed by three washes. Kinetoplasts and nuclei were then labeled with DAPI (10  $\mu$ g/mL) for 5min. Slides were washed three times with PBS and mounted with SlowFade Gold (Molecular probes). Single plane images were acquired with MetaMorph software on widefield Zeiss Imager Z1 or Axioplan 2 microscopes with a 100 $\times$  objective (NA 1.4) and processed without further treatment with ImageJ.

### 4.7 | Analysis of excreted end-products from the metabolism of carbon sources by proton <sup>1</sup>H-NMR

2 to  $4 \times 10^7$  *T. brucei* PCF, *Leishmania* promastigote or *T. congolense* BSF cells were collected by centrifugation at 1400 $\times$ g for 10min, washed twice with phosphate-buffered saline supplemented with 2g/L NaHCO<sub>3</sub> (pH7.4), and incubated in 1mL (single point analysis) of PBS supplemented with 2g/L NaHCO<sub>3</sub> (pH7.4). Cells were maintained for 6h at 27°C in incubation buffer containing one <sup>13</sup>C-enriched carbon source (1mM, [U-<sup>13</sup>C]-Glucose or [U-<sup>13</sup>C]-Glycerol or [U-<sup>13</sup>C]-Threonine; U stands for "uniformly <sup>13</sup>C-labeled"), except for *T. congolense* BSF, which were incubated for only 1h30 at 37°C. The integrity of the cells during the incubation was checked by microscopic observation. The supernatant (1mL) was collected and 50  $\mu$ L of maleate solution in Deuterated water (D<sub>2</sub>O; 10mM) was added as an internal reference. <sup>1</sup>H-NMR spectra were performed at 500.19MHz on a Bruker Avance III 500 HD spectrometer equipped with a 5mm cryoprobe Prodigy. Measurements were recorded at 25°C. Acquisition conditions were as follows: 90° flip angle, 5000Hz spectral width, 32K memory size, and 9.3s total recycle time. Measurements were performed with 64 scans for a total time close to 10min 30s.

## 4.8 | Cas9 cloning, expression and purification Cas9

The *eSpCas9(1.1)* gene containing two nuclear localization signals (NLS) was obtained from Addgene (Plasmid #71814) and cloned into the pST32 vector, which contains two N-terminal and C-terminal His-tag (Gift from Fanny Boissier, INSERM U1212 CNRS 5320, University of Bordeaux), using the *NcoI* and *EcoRI* restriction sites. A third nuclear localization signal (SV40) was added by hybridization of two complementary primers (Table S1) containing the SV40 NLS and cloned in frame at the 3' end of the pST32-*eSpCas9(1.1)* vector using *EcoRI* and *XhoI* restriction sites, generating the vector pST32-*eSpCas9(1.1)*-3NLS (Figure 1b). The plasmid was then transformed into *E. coli* Rosetta 2(DE3) competent cells (Novagen).

A bacterial preculture was grown overnight at 37°C with shaking and used to inoculate 100 mL of LB-Miller medium (peptone 10 g, yeast-extract 5 g, NaCl 10 g, pH 7). The culture was grown at 37°C with shaking to an optical density at 600 nm (OD<sub>600</sub>) of 0.6 to 0.8. Protein expression was induced by adding isopropyl-β-D-thiogalactopyranoside (IPTG; 100 μM), and the culture was kept at 18°C with shaking overnight. Cells were harvested by centrifugation, and the pellet was resuspended in 10 mL lysis buffer containing 500 mM KCl, 20 mM Hepes, 5 mM imidazole, pH 7.5 and protease inhibitor cocktail without EDTA (Merck). After lysis by sonication (20 sec, four times), the soluble fraction was obtained by centrifugation (30,000 × g, 30 min at 4°C) and purified by immobilized metal ion affinity chromatography (IMAC) using a His-Select Nickel Affinity Gel (Sigma) in a fast protein liquid chromatography (FPLC) system (ÄKTA; GE Healthcare Life Sciences). All chromatographic steps were performed at 4°C. 2 mL of His-Select Nickel resin were equilibrated in buffer and packed in a XK 10/50 mm column housing (Omnifit) with 20 mL lysis buffer. The cleared lysate was loaded on the column using a syringe at 1 mL/min rate. The column with bound protein was washed first with buffer (20 mM Hepes, 500 mM KCl, 50 mM imidazole, pH 7.5) until the absorbance returned to baseline again. The protein was eluted by applying a gradient from 0% to 100% elution buffer (20 mM Hepes, 500 mM KCl, 1 M imidazole, pH 7.5) over 20 mL and collected in 2 mL fractions. All peak fractions were analyzed for the presence of *eSpCas9(1.1)*-3NLS using SDS-PAGE, and the purity was estimated to be ~80% based on band intensity (Figure S1). An alternative to the ÄKTA purification was to purify the Cas9 protein in batches using Ni<sup>2+</sup>-resin and incubate for 30 min at 4°C. The resin was washed three times with 50 mM imidazole in 500 mM NaCl, Tris-HCl pH 8 and 3 times with 250 mM imidazole in 500 mM NaCl, Tris-HCl pH 8. *eSpCas9(1.1)*-3NLS was eluted with 500 mM imidazole in 500 mM NaCl, Tris-HCl pH 8. Fractions were analyzed by SDS-PAGE. The elution buffer was then exchanged for storage buffer (20 mM HEPES-KOH, 500 mM KCl, 1 mM DTT, pH 7.5) while concentrating the protein to a volume <1.5 mL using a 50,000 MWCO concentrator (Amicon) at 4000 × g. Buffer exchange prevented precipitation in the concentrator. The concentrated fraction was then centrifuged for 10 min at 16,900 × g at 4°C to remove all precipitated material. The protein concentration was determined

using a bicinchoninic acid (BCA) protein assay kit (Thermo Scientific), and the yield was determined to be approximately 5 mg/100 mL of bacteria culture.

## 4.9 | Statistical analysis

Experiments were performed at least in triplicates. Statistical analyses were performed using Prism (GraphPad) software. The results are presented as mean ± SD. A two-tailed student's *t*-test (unpaired, normal distribution, and parametric test) was used to determine statistical differences against the indicated group (confidence interval 95%—*p*-value style: 0.1234 (ns); 0.0332 (\*); 0.0021 (\*\*); 0.0002 (\*\*); <0.0001 (\*\*\*\*)).

## AUTHOR CONTRIBUTIONS

**Emmanuel Tetaud:** Conceptualization; methodology; formal analysis; supervision; validation; writing – original draft; writing – review and editing. **Corinne Asencio:** Methodology; formal analysis; writing – review and editing. **Perrine Hervé:** Methodology; formal analysis; writing – review and editing. **Pauline Morand:** Methodology; formal analysis. **Quentin Oliveres:** Methodology; formal analysis. **Chloé Alexandra Morel:** Methodology; formal analysis; writing – review and editing. **Valérie Prouzet-Mauleon:** Conceptualization; writing – review and editing. **Marc Biran:** Methodology; conceptualization; formal analysis; writing – review and editing. **Sarah Monic:** Methodology; formal analysis. **Mélanie Bonhivers:** Conceptualization; funding acquisition; writing – review and editing. **Derrick Roy Robinson:** Conceptualization; funding acquisition; writing – review and editing. **Marc Ouellette:** Conceptualization; writing – review and editing; supervision. **Loïc Rivière:** Conceptualization; writing – review and editing; supervision. **Frédéric Bringaud:** Conceptualization; funding acquisition; writing – original draft; validation; supervision; writing – review and editing.

## ACKNOWLEDGMENTS

Cell sorter analyses were performed at the TBMCore facility (FACSility) on BD FACSAria™ III Sorter and we thank Atika Zouine and Vincent Pitard for technical assistance, data acquisition, and interpretation (TBMCore CNRS 3427, INSERM US005, Université de Bordeaux). We also thank the CRISP'edit platform for their valuable advice during the setup of the CRISPR system. We thank Keith Gull (University of Manchester) for providing us with the anti-PFR antibody. The Bringaud and Robinson teams are supported by the Centre National de la Recherche Scientifique (CNRS, <https://www.cnrs.fr/>), the Université de Bordeaux (<https://www.u-bordeaux.fr/>) and the Agence Nationale de la Recherche (ANR, <https://anr.fr/>) through the ParaFrap "Laboratoire d'Excellence" (LabEx, <https://www.enseignementsup-recherche.gouv.fr/cid51355/laboratoires-d-excellence.html>) (ANR-11-LABX-0024). This work was supported by the "Fondation pour la Recherche Médicale" (FRM, <https://www.frm.org/>) ("Equipe FRM", grant n°EQU201903007845) and the ANR grant ADIPOTRYP (ANR19-CE15-0004-01) to FB, and by the ANR

grants Structu-Ring (ANR-20-CE91-0003) and Flagel-Ome (ANR-19-CE17-0014-03) to MB. MO is the holder of a Canada Research Chair and the recipient of a CIHR Foundation Grant. He was the holder of a University de Bordeaux IDEX fellowship.

### CONFLICT OF INTEREST STATEMENT

The authors declare that there is no conflict of interest.

### DATA AVAILABILITY STATEMENT

The data that support the findings of this study are openly available in [10.1101/2023.10.25.563974](https://doi.org/10.1101/2023.10.25.563974) at <https://biorxiv.org/cgi/content/short/2023.10.25.563974v1>.

### ETHICS STATEMENT

No human or animal subjects were used in this study.

### ORCID

Emmanuel Tetaud  <https://orcid.org/0000-0001-9575-8671>

### REFERENCES

- Allmann, S., Wargnies, M., Plazolles, N., Cahoreau, E., Biran, M., Morand, P. et al. (2021) Glycerol suppresses glucose consumption in trypanosomes through metabolic contest. *PLoS Biology*, 19, e3001359.
- Barrangou, R., Fremaux, C., Deveau, H., Richards, M., Boyaval, P., Moineau, S. et al. (2007) CRISPR provides acquired resistance against viruses in prokaryotes. *Science*, 315, 1709–1712.
- Beneke, T., Madden, R., Makin, L., Valli, J., Sunter, J. & Gluenz, E. (2017) A CRISPR Cas9 high-throughput genome editing toolkit for kinetoplasts. *Royal Society Open Science*, 4, 170095.
- Boutin, J., Rosier, J., Cappellen, D., Prat, F., Toutain, J., Pennamen, P. et al. (2021) CRISPR-Cas9 globin editing can induce megabase-scale copy-neutral losses of heterozygosity in hematopoietic cells. *Nature Communications*, 12, 4922.
- Bringaud, F., Biran, M., Millerioux, Y., Wargnies, M., Allmann, S. & Mazet, M. (2015) Combining reverse genetics and nuclear magnetic resonance-based metabolomics unravels trypanosome-specific metabolic pathways. *Molecular Microbiology*, 96, 917–926.
- Coustou, V., Plazolles, N., Guegan, F. & Baltz, T. (2012) Sialidases play a key role in infection and anaemia in *Trypanosoma congolense* animal trypanosomiasis. *Cellular Microbiology*, 14, 431–445.
- Crawford, E.D., Quan, J., Horst, J.A., Ebert, D., Wu, W. & Derisi, J.L. (2017) Plasmid-free CRISPR/Cas9 genome editing in *Plasmodium falciparum* confirms mutations conferring resistance to the dihydroisoquinoline clinical candidate SJ733. *PLoS ONE*, 12, e0178163.
- D'Astolfo, D.S., Pagliero, R.J., Pras, A., Karthaus, W.R., Clevers, H., Prasad, V. et al. (2015) Efficient intracellular delivery of native proteins. *Cell*, 161, 674–690.
- Desquesnes, M., Sazmand, A., Gonzatti, M., Boulange, A., Bossard, G., Thevenon, S. et al. (2022) Diagnosis of animal trypanosomes: proper use of current tools and future prospects. *Parasites & Vectors*, 15, 235.
- Engstler, M. & Beneke, T. (2023) Gene editing and scalable functional genomic screening in *Leishmania* species using the CRISPR/Cas9 cytosine base editor toolbox LeishBASEdit. *eLife*, 12, e85605.
- Espada, C.R., Quilles, J.C., Jr., Albuquerque-Wendt, A., Cruz, M.C., Beneke, T., Lorenzon, L.B. et al. (2021) Effective genome editing in *Leishmania (Viannia) braziliensis* stably expressing Cas9 and T7 RNA polymerase. *Frontiers in Cellular and Infection Microbiology*, 11, 772311.
- Fu, Y., Foden, J.A., Khayter, C., Maeder, M.L., Reyon, D., Joung, J.K. et al. (2013) High-frequency off-target mutagenesis induced by CRISPR-Cas nucleases in human cells. *Nature Biotechnology*, 31, 822–826.
- Gomaa, F., Li, Z.H., Beaudoin, D.J., Alzan, H., Girguis, P.R., Docampo, R. et al. (2022) CRISPR/Cas9-induced disruption of *Bodo saltans* paraflagellar rod-2 gene reveals its importance for cell survival. *Environmental Microbiology*, 24, 3051–3062.
- Imamura, H., Downing, T., Van Den Broeck, F., Sanders, M.J., Rijal, S., Sundar, S. et al. (2016) Evolutionary genomics of epidemic visceral leishmaniasis in the Indian subcontinent. *eLife*, 5, e12613.
- Inoue, N., Otsu, K., Ferraro, D.M. & Donelson, J.E. (2002) Tetracycline-regulated RNA interference in *Trypanosoma congolense*. *Molecular and Biochemical Parasitology*, 120, 309–313.
- Ishino, Y., Shinagawa, H., Makino, K., Amemura, M. & Nakata, A. (1987) Nucleotide sequence of the *iap* gene, responsible for alkaline phosphatase isozyme conversion in *Escherichia coli*, and identification of the gene product. *Journal of Bacteriology*, 169, 5429–5433.
- Jinek, M., Chylinski, K., Fonfara, I., Hauer, M., Doudna, J.A. & Charpentier, E. (2012) A programmable dual-RNA-guided DNA endonuclease in adaptive bacterial immunity. *Science*, 337, 816–821.
- Kim, S., Kim, D., Cho, S.W., Kim, J. & Kim, J.S. (2014) Highly efficient RNA-guided genome editing in human cells via delivery of purified Cas9 ribonucleoproteins. *Genome Research*, 24, 1012–1019.
- Kolev, N.G., Tschudi, C. & Ullu, E. (2011) RNA interference in protozoan parasites: achievements and challenges. *Eukaryotic Cell*, 10, 1156–1163.
- Kovarova, J., Novotna, M., Faria, J., Rico, E., Wallace, C., Zoltner, M. et al. (2022) CRISPR/Cas9-based precision tagging of essential genes in bloodstream form African trypanosomes. *Molecular and Biochemical Parasitology*, 249, 111476.
- Lander, N., Chiurillo, M.A., Storey, M., Vercesi, A.E. & Docampo, R. (2016) CRISPR/Cas9-mediated endogenous C-terminal tagging of *Trypanosoma cruzi* genes reveals the acidocalcisome localization of the inositol 1,4,5-trisphosphate receptor. *The Journal of Biological Chemistry*, 291, 25505–25515.
- Lander, N., Chiurillo, M.A., Vercesi, A.E. & Docampo, R. (2017) Endogenous C-terminal tagging by CRISPR/Cas9 in *Trypanosoma cruzi*. *Bio-Protocol*, 7, e2299.
- Lander, N., Li, Z.H., Niyogi, S. & Docampo, R. (2015) CRISPR/Cas9-induced disruption of paraflagellar rod protein 1 and 2 genes in *Trypanosoma cruzi* reveals their role in flagellar attachment. *MBio*, 6, e01012.
- Liang, X., Potter, J., Kumar, S., Zou, Y., Quintanilla, R., Sridharan, M. et al. (2015) Rapid and highly efficient mammalian cell engineering via Cas9 protein transfection. *Journal of Biotechnology*, 208, 44–53.
- Lye, L.F., Owens, K.L., Jang, S., Marcus, J.E., Brettmann, E.A. & Beverley, S.M. (2022) An RNA interference (RNAi) toolkit and its utility for functional genetic analysis of *Leishmania (Viannia)*. *Genes (Basel)*, 14, 93.
- Mannaert, A., Downing, T., Imamura, H. & Dujardin, J.C. (2012) Adaptive mechanisms in pathogens: universal aneuploidy in leishmania. *Trends in Parasitology*, 28, 370–376.
- Millerioux, Y., Mazet, M., Bouyssou, G., Allmann, S., Kiema, T.R., Bertiaux, E. et al. (2018) De novo biosynthesis of sterols and fatty acids in the *Trypanosoma brucei* procyclic form: carbon source preferences and metabolic flux redistributions. *PLoS Pathogens*, 14, e1007116.
- Minet, C., Chantal, I. & Berthier, D. (2023) Recent advances in genome editing of bloodstream forms of *Trypanosoma congolense* using CRISPR-Cas9 ribonucleoproteins: proof of concept. *Experimental Parasitology*, 252, 108589.
- Mojica, F.J., Diez-Villasenor, C., Garcia-Martinez, J. & Soria, E. (2005) Intervening sequences of regularly spaced prokaryotic repeats derive from foreign genetic elements. *Journal of Molecular Evolution*, 60, 174–182.
- Monic, S.G., Lamy, A., Thonnus, M., Bizarra-Rebello, T., Bringaud, F., Smith, T.K. et al. (2022) A novel lipase with dual localisation in *Trypanosoma brucei*. *Scientific Reports*, 12, 4766.
- Morel, C.A., Asencio, C., Blancard, C., Salin, B., Gontier, E., Duvezin-Caubet, S. et al. (2023) Identification of a novel and



- ancestral machinery involved in mitochondrial membrane branching in *Trypanosoma brucei*. *bioRxiv*. Available from: <https://doi.org/10.1101/2023.06.28.546890>
- Mozdy, A.D., Mccaffery, J.M. & Shaw, J.M. (2000) Dnm1p GTPase-mediated mitochondrial fission is a multi-step process requiring the novel integral membrane component Fis1p. *The Journal of Cell Biology*, 151, 367–380.
- Ngo, H., Tschudi, C., Gull, K. & Ullu, E. (1998) Double-stranded RNA induces mRNA degradation in *Trypanosoma brucei*. *Proceedings of the National Academy of Sciences of the United States of America*, 95, 14687–14692.
- Peng, D., Kurup, S.P., Yao, P.Y., Minning, T.A. & Tarleton, R.L. (2014) CRISPR-Cas9-mediated single-gene and gene family disruption in *Trypanosoma cruzi*. *MBio*, 6, e02097-14.
- Peng, D. & Tarleton, R. (2015) EuPagdt: a web tool tailored to design CRISPR guide RNAs for eukaryotic pathogens. *Microbial Genomics*, 1, e000033.
- Pineda, E., Thonnus, M., Mazet, M., Mourier, A., Cahoreau, E., Kulyk, H. et al. (2018) Glycerol supports growth of the *Trypanosoma brucei* bloodstream forms in the absence of glucose: analysis of metabolic adaptations on glycerol-rich conditions. *PLoS Pathogens*, 14, e1007412.
- Reis-Cunha, J.L., Valdivia, H.O. & Bartholomeu, D.C. (2018) Gene and chromosomal copy number variations as an adaptive mechanism towards a parasitic lifestyle in trypanosomatids. *Current Genomics*, 19, 87–97.
- Rico, E., Jeacock, L., Kovarova, J. & Horn, D. (2018) Inducible high-efficiency CRISPR-Cas9-targeted gene editing and precision base editing in African trypanosomes. *Scientific Reports*, 8, 7960.
- Rogers, M.B., Hillel, J.D., Dickens, N.J., Wilkes, J., Bates, P.A., Depledge, D.P. et al. (2011) Chromosome and gene copy number variation allow major structural change between species and strains of *Leishmania*. *Genome Research*, 21, 2129–2142.
- Ryan, O.W., Skerker, J.M., Maurer, M.J., Li, X., Tsai, J.C., Poddar, S. et al. (2014) Selection of chromosomal DNA libraries using a multiplex CRISPR system. *eLife*, 3, e03703.
- Shaw, S., Knusel, S., Hoenner, S. & Roditi, I. (2020) A transient CRISPR/Cas9 expression system for genome editing in *Trypanosoma brucei*. *BMC Research Notes*, 13, 268.
- Slaymaker, I.M., Gao, L., Zetsche, B., Scott, D.A., Yan, W.X. & Zhang, F. (2016) Rationally engineered Cas9 nucleases with improved specificity. *Science*, 351, 84–88.
- Soares Medeiros, L.C., South, L., Peng, D., Bustamante, J.M., Wang, W., Bunkofsky, M. et al. (2017) Rapid, selection-free, high-efficiency genome editing in protozoan parasites using CRISPR-Cas9 ribonucleoproteins. *MBio*, 8, e01788-17.
- Solleis, L., Ghorbal, M., Macpherson, C.R., Martins, R.M., Kuk, N., Crobu, L. et al. (2015) First efficient CRISPR-Cas9-mediated genome editing in leishmania parasites. *Cellular Microbiology*, 17, 1405–1412.
- Toukara, M., Boulange, A., Thonnus, M., Bringaud, F., Belem, A.M.G., Bengaly, Z. et al. (2021) Novel protein candidates for serodiagnosis of African animal trypanosomiasis: evaluation of the diagnostic potential of lysophospholipase and glycerol kinase from *Trypanosoma brucei*. *PLoS Neglected Tropical Diseases*, 15, e0009985.
- Tovar, J., Wilkinson, S., Mottram, J.C. & Fairlamb, A.H. (1998) Evidence that trypanothione reductase is an essential enzyme in leishmania by targeted replacement of the tryA gene locus. *Molecular Microbiology*, 29, 653–660.
- Wargnies, M., Bertiaux, E., Cahoreau, E., Ziebart, N., Cruzols, A., Morand, P. et al. (2018) Gluconeogenesis is essential for trypanosome development in the tsetse fly vector. *PLoS Pathogens*, 14, e1007502.
- Zhang, W.W., Lypaczewski, P. & Matlashewski, G. (2017) Optimized CRISPR-Cas9 genome editing for *Leishmania* and its use to target a multigene family, induce chromosomal translocation, and study DNA break repair mechanisms. *mSphere*, 2, e00340-16.
- Zhang, W.W. & Matlashewski, G. (2015) CRISPR-Cas9-mediated genome editing in *Leishmania donovani*. *MBio*, 6, e00861.

## SUPPORTING INFORMATION

Additional supporting information can be found online in the Supporting Information section at the end of this article.

**How to cite this article:** Asencio, C., Hervé, P., Morand, P., Oliveres, Q., Morel, C.A., Prouzet-Mauleon, V. et al. (2024) *Streptococcus pyogenes* Cas9 ribonucleoprotein delivery for efficient, rapid and marker-free gene editing in *Trypanosoma* and *Leishmania*. *Molecular Microbiology*, 121, 1079–1094. Available from: <https://doi.org/10.1111/mmi.15256>